Molten salt synthesis and luminescence properties of Sm^{3+} doped $K_2LaNb_5O_{15}$ niobate phosphor

BING HAN*, YAWEI CHEN, BEIBEI LIU, JIE ZHANG

School of Material and Chemical Engineering, Zhengzhou University of Light Industry, Zhengzhou 450002, People's Republic of China

A series of polycrystalline powders Sm^{3+} doped $K_2LaNb_5O_{15}$ niobate phosphors were synthesized by molten salt method, and their phase purity and structures were investigated by powder X-ray diffraction. The as-prepared $K_2LaNb_5O_{15}$:Sm^{3+} samples exhibited a single phase tetragonal tungsten bronze (TTB) structure. Upon excitation with 407 nm, these phosphors presented orange-red emission and millisecond-level lifetime due to the intra-4f transitions of Sm^{3+} ions. According to the concentration dependent photoluminescence properties of the as-prepared phosphors, the optimal concentration of Sm^{3+} was confirmed to be 4%, and the concentration quenching phenomenon was originated from dipole–dipole interaction between Sm^{3+} ions. The results indicate the molten salt method is an efficient method to prepare $K_2LaNb_5O_{15}$-based phosphors at relatively low temperature, and $K_2LaNb_5O_{15}$:Sm^{3+} phosphor may be potential orange-red phosphor for solid state lighting.

(Received January 25, 2021; accepted April 8, 2022)

Keywords: Molten salt, Niobate; Sm^{3+}, Luminescence

1. Introduction

Among several rare earth ions, Sm^{3+} ion has rich energy level structure and can emit orange-red light in visible range upon excitation with UV or near-UV light. On the basis of the spectral characteristic of Sm^{3+}, Sm^{3+} doped inorganic phosphors are often considered as the potential orange-red component for application in white light-emitting diodes, which have been currently considered as the most promising solid state lighting technology in 21st century [1,2]. Thus, many novel orange-red phosphors based on Sm^{3+}-doping have been recently exploited, such as $Mg_3YGe_3O_{12}$:xSm^{3+} [3], $K_5Y(P_2O_7)_2$:Sm^{3+} [4], $Ca_9Gd(PO_4)_7$:Sm^{3+} [5], $Sr_9In(PO_4)_7$:Sm^{3+} [6].

Due to the desirable high temperature stabilities and relatively low phonon energy, the tetragonal tungsten bronze-type (TTB-type) niobate compounds are considered as the promising host materials for phosphors. $K_2LaNb_5O_{15}$, a typical TTB-type niobate compound, crystallized in tetragonal structure, which comprises a complex array of $(Nb1/Nb2)O_6$ octahedra sharing corners in which three different types of tunnels for cations are formed [7,8]. The luminescence properties of Eu^{3+} doped $K_2LaNb_5O_{15}$ red phosphors have been reported by Mackevic et al. [9] and Hou et al. [10], in which the conventional high-temperature solid state method is utilized with sintering temperature of 1300℃.

Among numerous inorganic-synthesis methods, molten salt method is an important method that utilizes molten salt as the reaction medium to enable molecular-level mixing of different component oxides, and results in homogeneous structure of the desired product [11,12]. Compared with conventional high-temperature solid state method, molten salt method is provided with unique advantages such as low reaction temperature, short reaction time, less aggregation of particles and etc. [13]. Thus, molten salt method attracts much attention nowadays in the synthesis of different types of inorganic phosphor [14,15]. However, to our knowledge, the molten salt synthesis and luminescence properties of Sm^{3+} doped $K_2LaNb_5O_{15}$ phosphors have not been still

reported up to date. In this work, Sm^{3+} doped $K_2LaNb_5O_{15}$ phosphors were synthesized by molten salt method at relatively low temperature for the first time, and their luminescence properties were investigated.

2. Experimental section

A series of Sm^{3+} doped $K_2LaNb_5O_{15}$ phosphors [$K_2La_{1-x}Sm_xNb_5O_{15}$ (x = 0.005, 0.01, 0.02, 0.04, 0.06, 0.08)] were successfully synthesized by molten salt method. The starting materials are K_2CO_3 (A.R.), KCl (A.R.), Nb_2O_5 (99.99%), La_2O_3 (99.99%), Sm_2O_3 (99.99%), in which KCl is used as the material of molten salt. The weight ratio of KCl to oxides to is 1:2. All stoichiometric reagents as well as KCl are accurately weighed and adequately mixed in alcohol by continuous grinding. Then, the mixture was transferred to an alumina crucible and calcined at 900 ℃ for 2 h in air. After the obtained products were cooled naturally to room temperature, they were washed with distilled water several times to remove the residual KCl. Finally, the products were dried at 100 °C for 12 h and ground again into fine particles for the next characterizations.

The X-ray diffraction (XRD) patterns of the products were collected in an X-Ray Diffractometer (Bruker D8) with Cu Kα (λ = 1.5405 Å) radiation. The morphology and size of the sintered particles were observed with a scanning electron microscope (SEM, JSM-6490LV). Photoluminescence (PL) spectra and decay curves were recorded with a Combined Fluorescence Lifetime&Steady State Fluorescence Spectrometer (EDINBURGH FLS980) with a 450W xenon lamp and a 100W μF2 microsecond flash lamp as the excitation source, respectively.

3. Results and discussion

The XRD patterns of $K_2La_{1-x}Sm_xNb_5O_{15}$ (x = 0.005, 0.04, and 0.08) as representatives are shown in Fig. 1. It can be obviously observed that all the diffraction peaks of the as-prepared phosphors are similar with each other in shape and location, and in agreement with the Joint Committee on Powder Diffraction Strands card data [JCPDS#39–1442] of $K_2LaNb_5O_{15}$. No extra impurity phase can be observed, indicating that the doping of Sm^{3+} does not influence largely on the host structure due to the similar ionic radius and same valence state of La^{3+} and Sm^{3+}. The XRD result illustrates the single-phase $K_2LaNb_5O_{15}$:Sm^{3+} phosphors with TTB-type structure are successfully synthesized by molten salt method. The synthesis temperature (900 ℃) and time (2 h) in current work are less largely than that for the preparation of $K_2LaNb_5O_{15}$:Eu^{3+} phosphors by conventional high-temperature solid-state method [9,10], which is advantageous to the energy-conservation and environment-protection in current society.

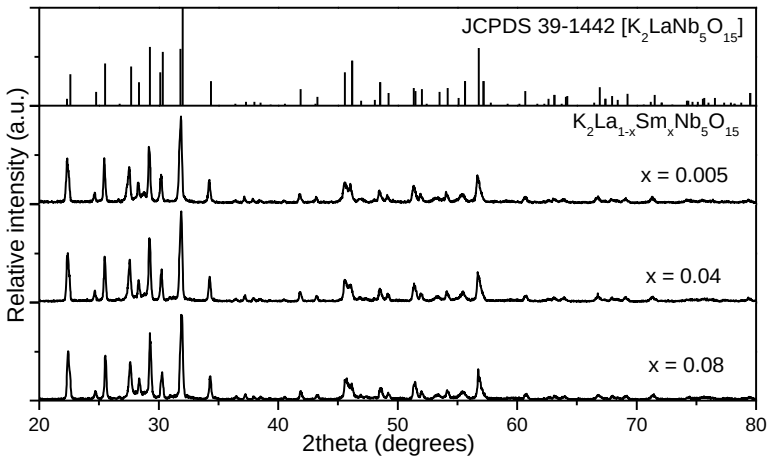

Fig. 1 XRD patterns of $K_2La_{1-x}Sm_xNb_5O_{15}$ (x = 0.005, 0.04, and 0.08)

Fig. 2 shows the SEM image of sample $K_2La_{1-x}Sm_xNb_5O_{15}$ (x = 0.04), in which obvious agglomeration and irregular shape are observed. The particle size could be in micrometer range.

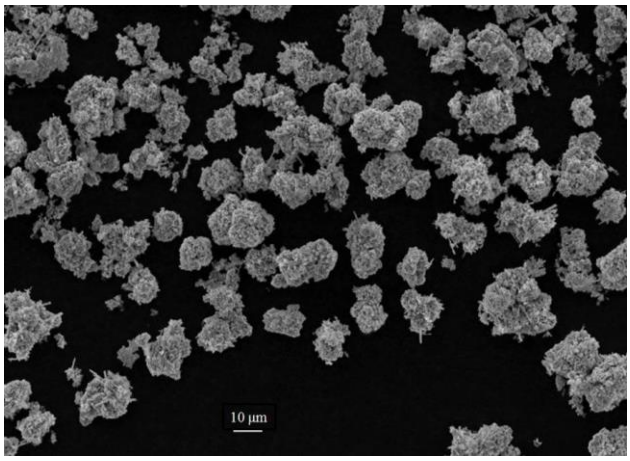

Fig. 2 SEM image of sample $K_2La_{1-x}Sm_xNb_5O_{15}$ (x = 0.04)

Fig. 3 shows the photoluminescence excitation (a) and emission (b) spectra of sample $K_2La_{1-x}Sm_xNb_5O_{15}$ (x = 0.04). In the excitation spectrum (a) by monitoring 599 nm emission, a series of sharp peaks are observed, which are assigned to $^6H_{5/2}\rightarrow{}^6P_{7/2}$ (～379 nm), $^6H_{5/2}\rightarrow{}^4F_{7/2}$ (407 nm), $^6H_{5/2}\rightarrow{}^6P_{5/2}$ (420 nm) transitions of Sm^{3+} ions [5]. Among them, the $^6H_{5/2}\rightarrow{}^4F_{7/2}$ transition at 407 nm is with highest excitation intensity, which is similar with that in other Sm^{3+} doped phosphors such as $K_5Y(P_2O_7)_2:Sm^{3+}$ [4], $Sr_9In(PO_4)_7:Sm^{3+}$ [6], and $Na_5Bi(P_2O_7)_2:Sm^{3+}$ [16]. The excitation characteristic obtained indicates the current phosphor can be excited by near-UV chips in the phosphor-converted w-LEDs. Under 407 nm excitation, the emission spectrum (b) presents four emission peaks at 564 nm, 599 nm, 645 nm, and 709 nm, which are undoubtedly due to the $^4G_{5/2}\rightarrow{}^6H_{5/2}$, $^4G_{5/2}\rightarrow{}^6H_{7/2}$, $^4G_{5/2}\rightarrow{}^6H_{9/2}$, and $^4G_{5/2}\rightarrow{}^6H_{11/2}$ transitions of Sm^{3+} ions [3]. Obviously, the purely electric dipole (ED) transition $^4G_{5/2}\rightarrow{}^6H_{9/2}$ (645 nm) is stronger than the purely magnetic dipole (MD) transition $^4G_{5/2}\rightarrow{}^6H_{5/2}$, indicating that Sm^{3+} ions locate low symmetry sites in $K_2LaNb_5O_{15}$ host [17]. The CIE chromaticity coordinate (x, y) of sample $K_2La_{1-x}Sm_xNb_5O_{15}$ (x = 0.04) is calculated and shown in Fig. 3(c). The obtained values are (0.591, 0.403), and located in the orange-red region.

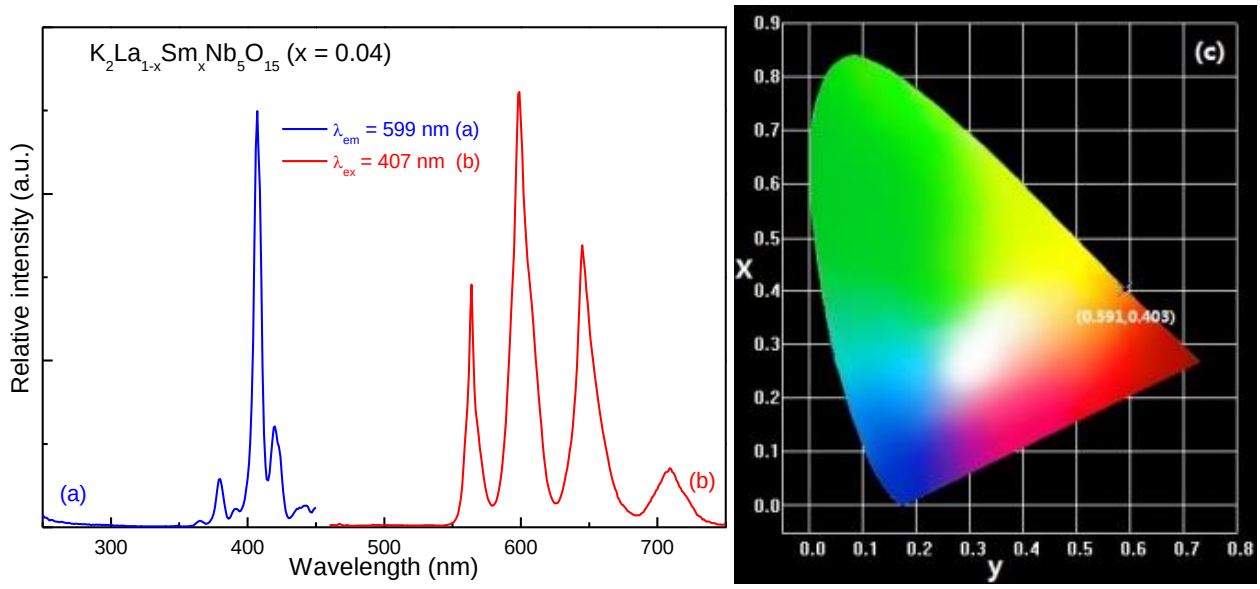

Fig. 3 Photoluminescence excitation (a) and emission (b) spectra of sample $K_2La_{1-x}Sm_xNb_5O_{15}$ (x = 0.04) (color online)

To investigate the effect of Sm^{3+} concentration on the luminescence properties of $K_2LaNb_5O_{15}:Sm^{3+}$ phosphors, the emission spectra of $K_2La_{1-x}Sm_xNb_5O_{15}$ (x = 0.005-0.08) phosphors upon excitation with 407 nm are shown in Fig. 4. It is obvious that the spectral distribution does not change with the increase of Sm^{3+} concentration. However, the concentration quenching phenomenon of Sm^{3+} can be easily observed, as shown in the inset of Fig. 4. When the concentration of Sm^{3+} exceed x = 0.04, the emission intensity decreases due to the non-radiative energy transfer between Sm^{3+} ions [3,5].

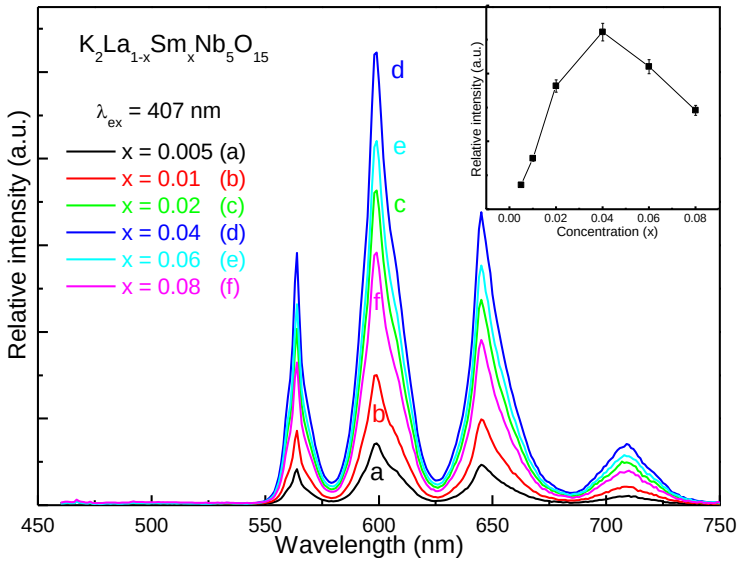

Fig. 4 Emission spectra of $K_2La_{1-x}Sm_xNb_5O_{15}$ (x = 0.005-0.08) phosphors upon excitation with 407 nm (color online)

In order to study the concentration quenching mechanism of Sm^{3+} in $K_2LaNb_5O_{15}$ host, the critical distance (R_c) of neighboring Sm^{3+} ions can be estimated based on the equation as follows [18],

$$R_c \approx 2\left(\frac{3V}{4\pi Z x_c}\right)^{1/3} \quad (1)$$

where V is the unit cell volume, Z is the number of the unit cell and x_c is the optimal concentration of activator ions. By using the crystal structure data (V = 618.3 $Å^3$, Z = 2) reported by Zhang et al. [7] as well as the optimal concentration of Sm^{3+} (x = 0.04) obtained in this work, the critical distance R_c is found to be 24.53 Å. The obtained R_c far exceed 5 Å and indicates that the electric multipolar interaction (not exchange interaction) is the predominant mechanism inducing the concentration quenching of Sm^{3+} [19].

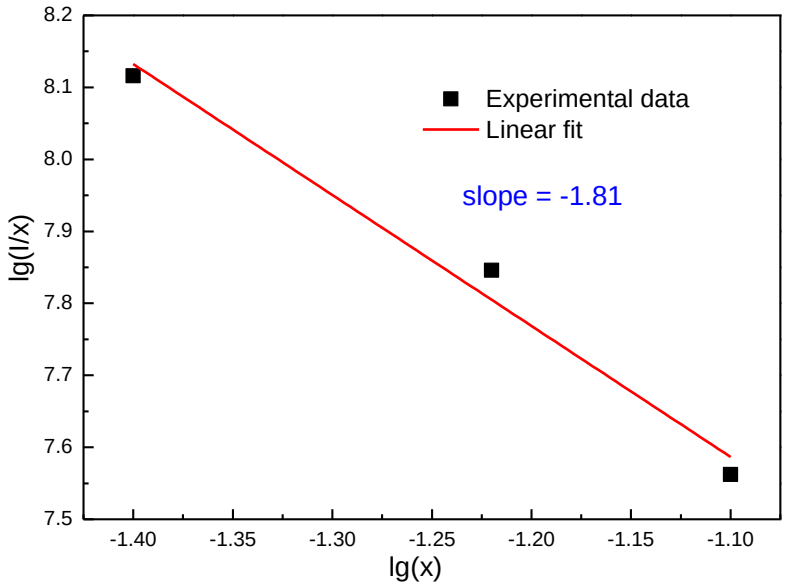

Fig. 5. Linear relationship between lg(I/x) and lg(x) in $K_2La_{1-x}Sm_xNb_5O_{15}$ (x = 0.04, 0.06, 0.08) (color online)

As is known to us, the multipolar interactions include quadrupole−quadrupole (q−q), dipole−dipole (d−d), and dipole−quadrupole (d−q) interactions. So, in order to confirm the specific type of electric multipolar interaction

for the concentration quenching of Sm^{3+}, the relationship between the emission intensity and the doping concentration can be investigated by using the following equation [20],

$$\frac{I}{x} = k[1 + \beta(x)^{\theta/3}]^{-1} \quad (2)$$

where I is the emission intensity, x is the concentration of activator not less than the optimal concentration, k and β are constants, and θ is the multipolar interaction constant (6 for d-d, 8 for d-q, and 10 for q-q, respectively). Because of $\beta(x)^{\theta/3} >> 1$, the linear relationship between lg(I/x) and lg(x) is investigated for $K_2LaNb_5O_{15}:Sm^{3+}$ phosphors under 407 nm excitation, as shown in Fig. 5. The slope (-θ/3) can be found to be -1.81, and thus the value of θ is calculated to be 5.43. The obtained result indicates that the concentration quenching phenomenon of Sm^{3+} ions in $K_2LaNb_5O_{15}$ host is mainly induced by the electric dipole-dipole interaction among Sm^{3+} ions. The similar results can be found in other Sm^{3+} doped phosphors [3,4,6,17].

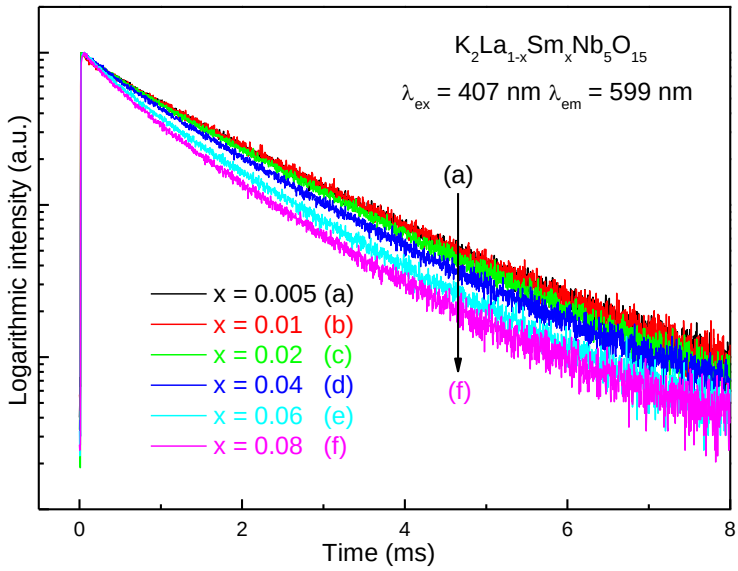

Fig. 6. Decay curves (λ_{ex} = 407 nm, λ_{em} = 599 nm) of samples $K_2La_{1-x}Sm_xNb_5O_{15}$ (x = 0.005-0.08) (color online)

The decay curves of samples $K_2La_{1-x}Sm_xNb_5O_{15}$ (x = 0.005-0.08) with appropriate parameters (λ_{ex} = 407 nm, λ_{em} = 599 nm) are measured and shown in Fig. 6. All decay curves can be well fitted with a two-exponential decay function as follows,

$$I_t = A_1 \exp\left(-\frac{t}{\tau_1}\right) + A_2 \exp\left(-\frac{t}{\tau_2}\right) + A_0 \quad (3)$$

where A_0, A_1 and A_2 are the fitting parameters; τ_1, τ_2 are the lifetimes for exponential components; t is the time. Then, the average decay time τ can be calculated in term of the following equation,

$$\tau = \frac{A_1\tau_1^2 + A_2\tau_2^2}{A_1\tau_1 + A_2\tau_2} \quad (4)$$

The average decay times can be calculated to be 1.42 ms, 1.40 ms, 1.34 ms, 1.21 ms, 1.03 ms, and 0.93 ms with x = 0.005-0.08 for samples $K_2La_{1-x}Sm_xNb_5O_{15}$. All the lifetime values are within milliseconds due to the forbidden nature of the 4f–4f transition of Sm^{3+} [6]. Moreover, with the increase in Sm^{3+}-concentration (x value), the lifetime decreases monotonously, indicating that the non-radiative energy transfer among Sm^{3+} become more efficient.

4. Conclusion

In summary, a series of novel orange-red emitting niobate phosphors $K_2LaNb_5O_{15}:Sm^{3+}$ were successfully prepared via molten salt method at 900 ℃. The XRD results indicated the as-prepared phosphors crystallized in single-phase TTB structure. The strongest excitation peak located at 407 nm, which was due to $^6H_{5/2} \rightarrow {}^4F_{7/2}$ transition of Sm^{3+}. Under 407 nm excitation, the characteristic $^4G_{5/2} \rightarrow {}^6H_J$ (J = 5/2, 7/2, 9/2, and 11/2) transitions of Sm^{3+} induced the orange-red emission of the as-prepared phosphors. With the

increase in the doping concentration of Sm^{3+}, the concentration quenching phenomenon was observed, which resulted from the electric dipole-dipole interaction among Sm^{3+} ions. In addition, the millisecond-level lifetimes for the as-prepared phosphors were obtained because of the forbidden nature of the 4f–4f transition of Sm^{3+}. The results showed that orange-red emitting $K_2LaNb_5O_{15}$:Sm^{3+} phosphors may have potential application in w-LEDs.

Acknowledgements

The work is financially supported by the National Natural Science Foundation of China (No. 21501153), and the Training Programme for Young Backbone Teacher in University of He'nan Province (No. 2017GGJS092).

References

[1] Y. Wei, H. Yang, Z. Y. Gao, G. C. Xing, M. S. Molokeev, G. G. Li, Chem. Commun. **56**, 9170 (2020).

[2] P. Gaffuri, M. Salaün, I. Gautier-Luneau, G. Chadeyron, A. Potdevin, L. Rapenne, E. Appert, V. Consonni, A. Ibanez, J. Mater. Chem. C **8**, 11839 (2020).

[3] C. Y. Ji, Z. Huang, X. Y. Tian, H. P. He, J. Wen, Y. X. Peng, J. Alloys Compd. **825**, 154176 (2020).

[4] L. Y. Shi, D. Zhao, Y. L. Xue, Y. C. Fan, R. J. Zhang, S. R. Zhang, J. Mater. Sci.: Mater. Electron. **31**, 15644 (2020).

[5] A. Siwach, M. Dalal, M. Dahiya, D. Kumar, J. Mater. Sci.: Mater. Electron. **31**, 13796 (2020).

[6] K. Su, Q. X. Zhang, X. N. Yang, B. Ma, J. Phys. D: Appl. Phys. **53**, 385101 (2020).

[7] W. Zhang, N. Kumada, T. Takei, Y. Yonesaki, N. Kinomura, Mater. Res. Bull. **42**, 844 (2007).

[8] M. Z. Li, Y. Shi, C. Z. Zhao, F. M. Yang, Q. Y. Li, X. X. Zhang, S. C. Wu, H. Y. Chen, J. M. Liu, T. Wei, Dalton Trans. **47**, 11337 (2018).

[9] I. Mackevic, J. Grigorjevaite, M. Janulevicius, A. Linkeviciute, S. Sakirzanovas, A. Katelnikovas, Opt. Mater. **89**, 25 (2019).

[10] J. S. Hou, P. Chen, G. H. Zhang, Y. Z. Fang, W. Z. Jiang, F. Q. Huang, Z. F. Ma, J. Lumin. **146**, 97 (2014).

[11] R. Liu, Y. Jin, L. J. Liu, Y. S. Liu, D. Tu, J. Alloys Compd. **826**, 154187 (2020).

[12] Y. Tian, Y. H. Fang, B. N. Tian, C. E. Cui, P. Huang, L. Wang, H. Y. Jia, B. J. Chen, J. Mater. Sci. **50**, 6060 (2015).

[13] S. Katyayan, S. Agrawal, J. Mater. Sci.: Mater. Electron. **31**, 8472 (2020).

[14] Y. H. Guo, S. H. Zhou, X. K. Sun, X. D. Lao, H. L. Yuan, J. Lumin. **211**, 271 (2019).

[15] C. Liu, C. G. Lyu, Y. F. Liu, Y. N. Lyu, J. Mater. Sci.: Mater. Electron. **27**, 10473 (2016).

[16] D. Zhao, X. Y. Han, Y. L. Xue, R. J. Zhang, S. R. Zhang, Y. N. Li, J. Mater. Sci.: Mater. Electron. **31**, 9911 (2020).

[17] Y. V. Baklanova, L.G. Maksimova, O. A. Lipina, A. P. Tyutyunnik, V. G. Zubkov, J. Lumin. **224**, 117315 (2020).

[18] G. Blasse, Phys. Lett. A **28**, 444 (1968).

[19] D. L. Dexter, J. Chem. Phys. **21**, 836 (1953).

[20] I. G. Van Uitert, J. Electrochem. Soc. **114**, 1048 (1967).

*Corresponding author: hanbing@zzuli.edu.cn